


 Cite this: *RSC Adv.*, 2021, 11, 35653

Formation of double emulsion micro-droplets in a microfluidic device using a partially hydrophilic–hydrophobic surface

 Ampol Kamnerdsook,^a Ekachai Juntasaro,^b *^a Numfon Khemthongcharoen,^b Mayuree Chanasakulniyom,^c Witsaroot Sripumkhai,^d Pattaraluck Pattamang,^d Chamras Promptmas,^b ^b Nithi Atthi^d and Wutthinan Jeamsaksiri^d

The objective of this paper is to propose a surface modification method for preparing PDMS microfluidic devices with partially hydrophilic–hydrophobic surfaces for generating double emulsion droplets. The device is designed to be easy to use without any complicated preparation process and also to achieve high droplet encapsulation efficiency compared to conventional devices. The key component of this preparation process is the permanent chemical coating for which the Pluronic surfactant is added into the bulk PDMS. The addition of Pluronic surfactant can modify the surface property of PDMS from a fully hydrophobic surface to a partially hydrophilic–hydrophobic surface whose property can be either hydrophilic or hydrophobic depending on the air- or water-treatment condition. In order to control the surface wettability, this microfluidic device with the partially hydrophilic–hydrophobic surface undergoes water treatment by injecting deionized water into the specific microchannels where their surface property changes to hydrophilic. This microfluidic device is tested by generating monodisperse water-in-oil-in-water (w/o/w) double emulsion micro-droplets for which the maximum droplet encapsulation efficiency of 92.4% is achieved with the average outer and inner diameters of 75.0 and 57.7 μm , respectively.

 Received 14th September 2021
 Accepted 26th October 2021

DOI: 10.1039/d1ra06887c

rsc.li/rsc-advances

Introduction

Double emulsion droplets are widely used in medicine, cosmetics, food and agriculture because only a small amount of chemicals is required for usage in the form of a multilayer emulsion. Additionally, double emulsion droplets can be used for encapsulation of various bioactive agents such as cells, bio-reagents and drugs. This is because their size and composition can be precisely controlled with preserved condition. Therefore, double emulsion droplets have been widely used in various biomedical applications such as drug delivery,^{1–3} cell biology,^{4–8} chemical reaction^{9,10} and microparticle production.^{11–15}

Droplets are made of two immiscible fluids: the dispersed fluid (core) and the continuous fluid (shell). The principle used for droplet generation is based on the shear stress that can

make droplet breakup. In general, there are two main methods for droplet generation: membrane emulsification^{16–18} and microfluidics. For membrane emulsification method, the dispersed fluid is injected directly into the continuous fluid so that the large number of droplets can be effectively produced. However, it is difficult for membrane emulsification to control the droplet size and to obtain the high efficiency of encapsulation because the shear stress can only be regulated by the dispersed fluid. For microfluidics, microfabrication can be used to make microfluidic devices and mass production of micro-droplets can be effectively made with high precision in the droplet size as well as high efficiency encapsulation by controlling the liquid flow rates of dispersed and continuous phases along micro-channels. With microfluidics, the droplet generation is based on two sources of shear stress to make droplet breakup at the micro-channel junction: one from the continuous fluid and the other one from the difference between the surface wettability of the dispersed fluid and the surface condition of the micro-channel. Therefore, microfluidics is more effective for double emulsion droplet generation than membrane emulsification.

The micro-channel used to generate droplets in microfluidics can be classified into 3 types: T-junction, flow-focusing and co-flow. The T-junction micro-channel^{19–21} is the simplest one where the continuous phase flows along the main micro-channel while the dispersed phase flows along the micro-

^aMechanical Engineering Simulation and Design Group, The Sirindhorn International Thai-German Graduate School of Engineering (TGGS), King Mongkut's University of Technology North Bangkok, Bangkok, 10800, Thailand. E-mail: ekachai.j@tggs.kmutnb.ac.th

^bDepartment of Biomedical Engineering, Faculty of Engineering, Mahidol University, Nakhon Pathom, 73170, Thailand

^cDepartment of Clinical Chemistry, Faculty of Medical Technology, Mahidol University, Nakhon Pathom, 73170, Thailand

^dThai Microelectronics Center (TMEC), National Electronics and Computer Technology Center, National Science and Technology Development Agency, Chachoengsao, 24000, Thailand



channel branch that makes the angle of 90° with the main micro-channel. The droplets are generated at the micro-channel junction. The T-junction micro-channel was then replaced by the flow-focusing micro-channel.^{22–39} For flow-focusing micro-channels, there are two micro-channel branches for continuous phase that make the angle of 90° with the main micro-channel of the dispersed phase at the micro-channel junction so that the shear stress of the continuous phase is balanced at the junction. This results in higher efficiency of droplet generation compared to that of the T-junction micro-channel. For co-flow micro-channels,^{40–47} the dispersed phase flows along the capillary tube inside the micro-channel of the continuous phase similar to annular tubes so that the dispersed and continuous phases flow in parallel. With higher friction inside the capillary tube, the dispersed phase flows at the lower speed compared to the continuous phase and experiences the shear stress from the continuous phase. Therefore, the droplet breakup takes place at the outlet of the capillary tube. The co-flow micro-channel is as efficient as the flow-focusing micro-channel to generate droplets with a wider variety of materials to make the co-flow micro-channels. However, the generation of double emulsion droplets requires micro-channels with both hydrophobic and hydrophilic surfaces in single microfluidic device. In general, if the water contact angle (WCA) is smaller than 90° , the surface is considered hydrophobic. If the WCA is greater than 90° , the surface is considered hydrophilic. For instance, the hydrophobic surface is used first to produce the water-in-oil (w/o) droplets while the hydrophilic surface is used later to produce the water-in-oil-in-water (w/o/w) droplets. Therefore, the surface modification, which is a simple and convenient method, is required for both microfluidic device fabrication and rapid droplet generation. The flow-focusing micro-channel is thus one of the most suitable choices for the generation of double emulsion droplets because it is more efficient than the T-junction micro-channel and more convenient for surface modification compared to the co-flow micro-channel.

There are various methods for surface modification to convert the hydrophobic surface to the hydrophilic surface for double emulsion droplet generation. The graft polymerization of acrylic acid is one of the surface modification methods that flows the acrylic acid solution into the micro-channel. The specific surface that needs modification is exposed to the ultraviolet (UV) light in order to obtain the hydrophilic surface while the rest of the surface is protected by the black electrical tape. After that, the surface is washed by the deionized water (DIW). With this method, the hydrophobic properties with WCA of 73° is obtained and the stability of surface properties can be maintained more than 10 weeks.^{22,26,32} Typically, the oxygen plasma is used to treat the polydimethylsiloxane (PDMS) surface. It is a simple and effective method to convert the hydrophobic surface to the hydrophilic surface with low WCA of less than 20° . However, the hydrophilic surface can be maintained up to 48 hours. Consequently, this method is not attractive for modifying the surface of double emulsion droplet generation devices.²³ However, the oxygen plasma can be used in an area-specific manner by using epoxy glue to block the micro-channel inlet beyond which the hydrophobic surface is

not modified.³⁴ The chemical coating is another commonly used method that flows a surfactant solution through the micro-channel in order to reduce the surface tension of the target surface and hence converting to hydrophilic surface. This is an effective method and its hydrophilic surface duration can maintain more longer than that of the oxygen plasma method.^{27–31,35–37} When the chemical coating solution is used to coat the surface to form the layer-by-layer deposition, the property duration is approximately one month before returning to the hydrophobic surface.²⁵ Since only some selected surfaces require the surface modification, its process and technique for preparing such a device are rather complicated and not convenient. The multilayer geometry method is also interesting where the micro-channel network is fabricated with different surface properties in separate layers. It is simply to indicate the modified surface that can be used for droplet formation with more than two layers of droplet emulsion. However, it requires advanced fabrication technology to fabricate and align such a device in a micrometer scale. Hence, it is not a suitable method to produce the droplet size smaller than $100\ \mu\text{m}$.³⁸

Wu and Hjort (2009) studied the surface modification method for PDMS using the gradient-induced migration of embedded Pluronic. The surfactant solution is mixed with bulk PDMS during the fabrication process. This method is able to convert the surface properties from hydrophobic to hydrophilic. It is able to activate the surface modification by reacting to the solution that flows through the micro-channel network. In other words, when the water flows through the micro-channel, the Pluronic F-127 molecules migrate to the wetted surface of the micro-channel and convert the surface properties from hydrophobic to hydrophilic. After that, if the micro-channel is exposed to ambient air, the hydrophilic surface begins to return to the hydrophobic one again.⁴⁸ This method can easily control different surface properties and has longer stability of the surface wettability. Therefore, this method is attractive for the double emulsion droplet generation device. The objective of this research work is to apply the surface modification method using the permanent chemical coating in the PDMS microfluidic device for the first time to generate the double emulsion micro-droplets with the flow-focusing channel technique. This microfluidic device is designed to be easy to use without any complicated preparation process with higher efficiency compared to other microfluidic devices.

Results and discussion

In this paper, double emulsion droplet generation is performed by using the microfluidic device that is fabricated by the surface modification using permanent chemical coating in order to obtain the partially hydrophilic–hydrophobic surface. This modified surface is capable of adapting its surface property according to the fluid property when the fluid flows through the micro-channel. For example, the surface property is hydrophobic when the fluid is oil whereas the surface property becomes hydrophilic when the fluid is water. Therefore, this surface modification strategy is useful for the fabrication of the microfluidic device that is applied to generate water-in-oil-in-



water double emulsion droplets. The surface wettability of the hydrophilic surface and the recovery of the hydrophobic surface are key factors to enhance the improvement of the microfluidic device to be more convenient and more effective for double emulsion droplet generation compared to the conventional method.

Effect of Pluronic surfactant solution concentration on PDMS surface properties

For the permanent chemical coating modification, Pluronic F-127 surfactant solution is mixed with bulk PDMS to modify the PDMS surface property from hydrophobic to partially hydrophilic–hydrophobic. The performance of this surface modification technique is evaluated by measuring the static contact angle of a water droplet (WCA) with the droplet volume of 5.0 μL on a $2 \times 2 \text{ cm}^2$ PDMS flat sheet with and without modification. The PDMS flat sheet is fabricated by soft lithographic process whereas the modified PDMS samples are fabricated by mixing a bulk PDMS with Pluronic F-127 surfactant solution at five different concentrations of 2, 4, 6, 8 and 10 $\mu\text{L g}^{-1}$. After the samples are fabricated, they are treated by the O_2 plasma for 2.30 min in order to have the same preparation process as those of the microfluidic device fabrication. Then, the samples are treated with two different conditions (type A: exposed to air and type W: immersed in water) at room temperature for 24 hours and the surface wettability is studied by WCA measurement where five samples are used to measure WCA in each condition with three repetitions while, for each sample, WCA is measured at four different positions and then averaged. The effects of the concentration of Pluronic F-127 surfactant solution on the PDMS surface properties is investigated. During the duration of measuring the WCA, all samples are exposed to the ambient air for 30 days in order to study the stability of the hydrophobicity of the PDMS surfaces.

Fig. 1(a) shows the WCA of type A samples after exposed to the ambient air for 30 days where A0 stands for the PDMS sample without surface modification while A2–A10 denote the PDMS samples with various surfactant solution concentrations. It is found that the WCA decreases with the increasing concentration

of surfactant solution. After 24 hours, the surface properties of all type A samples are hydrophilic where $\text{WCA} < 90^\circ$ because these surfaces are still under the influence of O_2 plasma treatment. After 48 hours, the effect of O_2 plasma treatment is considerably reduced so that the WCA of all type A samples rapidly increases. After 72 hours, the surface properties of the A0–A8 samples recover from hydrophilicity to hydrophobicity where the WCA is greater than 90° . After 72 hours, the effect of permanent chemical coating on surface properties becomes dominant only for the A10 sample because it still remains hydrophilic with the sufficiently large amount of surfactant to maintain the hydrophilic property. The surface wettability duration of the sample A10 can be stabilised up to 30 days.

In case of type W samples, the WCA measurement over 30 days is shown in Fig. 1(b) where W0 stands for the PDMS sample without surface modification while W2–W10 denote the PDMS samples with various surfactant solution concentrations. It is found that the WCA of all type W samples decreases with the increasing concentration of surfactant solution. After 24 hours, the surface properties of all type W samples are hydrophilic similar to the type A samples, but the WCA of the type W samples is lower at the corresponding concentrations because being immersed in water for 24 hours can enhance the surface wettability. Moreover, the influence of O_2 plasma treatment on the type W samples still remains so that the surface properties of the type W samples recover from hydrophilic to hydrophobic more slowly compared to those of the type A samples. After 72 hours, the effect of O_2 plasma treatment is significantly reduced, the surface properties of the samples W4–W10 still remain hydrophilic while the surface properties of the samples W0–W2 become hydrophobic. Therefore, mixing Pluronic surfactant solution with bulk PDMS at the concentration of at least $4 \mu\text{L g}^{-1}$ is sufficient for surface modification with permanent chemical coating. After 9 days, the surface properties of the sample W4 are no longer hydrophilic while the hydrophilic surfaces of the samples W6–W10 remain for 30 days.

From the results in Fig. 1, it is found that the surface properties of the PDMS samples W6–W10 (immersed in water for 24 hours) can be changed from hydrophobic to hydrophilic for 30 days when the Pluronic solution concentration is at least $6 \mu\text{L}$

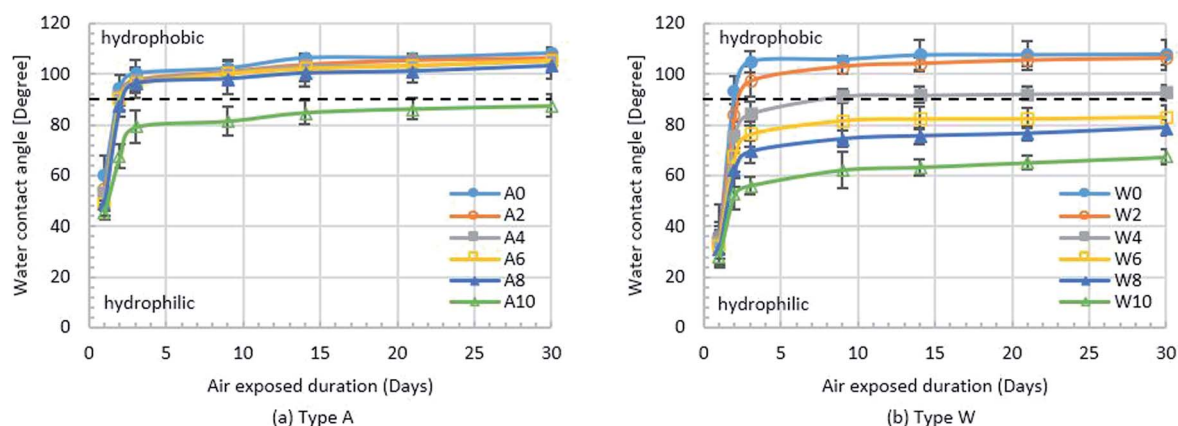


Fig. 1 Water contact angles of samples (a) type A: exposed to air and (b) type W: immersed in water. For WCA, the error bar is the corresponding standard deviation ($n = 3$) with the minimum and maximum values of 0.8% and 5.8%, respectively.



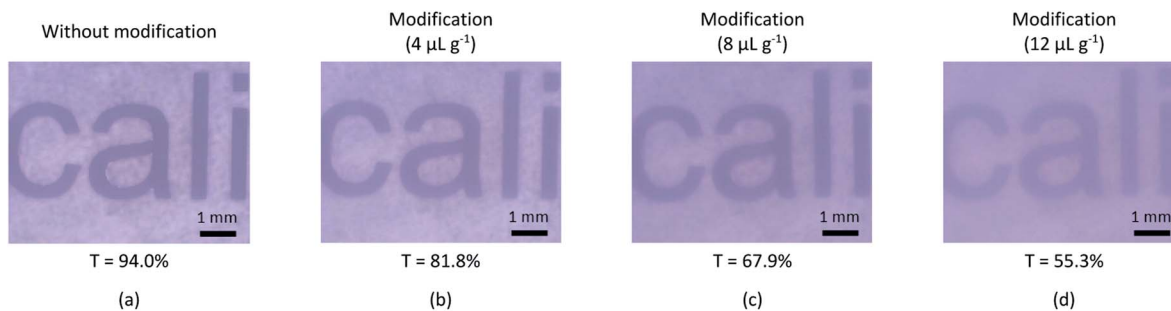


Fig. 2 Percent light transmission (%T) of PDMS samples (a) without surface modification and with surface modification using Pluronic F-127 surfactant solution of (b) $4 \mu\text{L g}^{-1}$, (c) $8 \mu\text{L g}^{-1}$ and (d) $12 \mu\text{L g}^{-1}$.

g^{-1} while the surface properties of the PDMS samples A0–A8 (exposed to air) return to hydrophobic after 48 hours when the Pluronic solution concentration is lower than $10 \mu\text{L g}^{-1}$. Clearly, the concentration of surfactant solution less than $4 \mu\text{L g}^{-1}$ cannot directly alter the surface wettability of PDMS but the water treatment can enable the surfactant solution to modify the PDMS surface. This is because when the Pluronic-modified sample is immersed in water, the oligomer of Pluronic migrates towards the wetted surface of that sample so that the surface property of that sample becomes hydrophilic. On the other hand, when the Pluronic-modified sample is exposed to air, the oligomer of PDMS migrates to replace the oligomer of Pluronic so that the contact angle increases and the surface property recovers to hydrophobic again.⁴⁸

However, an addition of Pluronic surfactant solution into PDMS deteriorates the optical transparency of PDMS and hence degrading the visualization quality when monitoring the fluid and micro-droplet behaviors inside the micro-channel. Fig. 2 shows the results of percent transmission (%T) of PDMS samples with and without surface modification at various surfactant

solution concentrations using the UV-visible spectrophotometer (Jasco, UV-2450) in a wave-length range of 400–800 nm and also their corresponding micrographs using optical microscope (OLYMPUS BX51M). It reveals that the higher concentration of Pluronic surfactant solution causes the lower percent transmission of PDMS samples. Therefore, an excessive amount of Pluronic surfactant solution can deteriorate the optical transparency of PDMS. It can be concluded that PDMS with Pluronic surfactant solution of $4 \mu\text{L g}^{-1}$ is the option to fabricate micro-fluidic devices for double emulsion droplet generation because its percent transmission is not much different (less than 10%) from that of PDMS without surface modification and its surface wettability can be altered by water treatment.

Pluronic modified PDMS with hydrophilic and hydrophobic surface control

For double emulsion droplet generation, both hydrophobic and hydrophilic surface types are required during the generation process. When the permanent chemical coating is used to

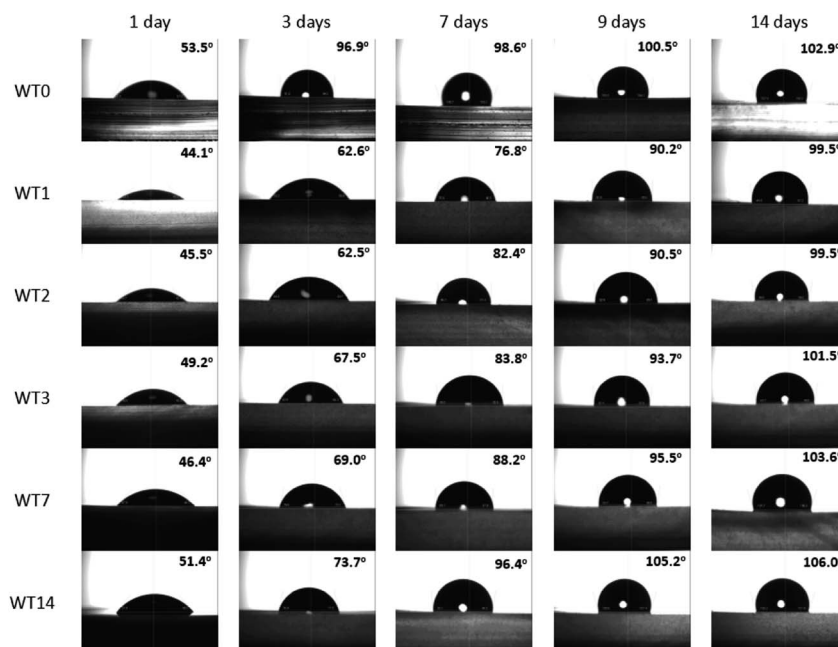


Fig. 3 Hydrophobic surface recovery of modified PDMS with Pluronic solution of $4.0 \mu\text{L g}^{-1}$: without water treatment (WT0) and with water treatment for 1, 2, 3, 7 and 14 days (WT1, WT2, WT3, WT7 and WT14).



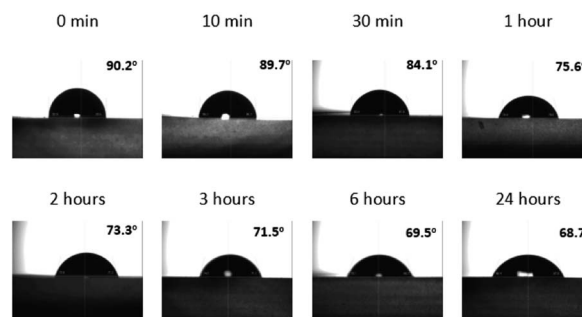
Table 1 Duration of hydrophilicity and hydrophobicity of modified PDMS with Pluronic solution of $4.0 \mu\text{L g}^{-1}$

Sample	Duration of hydrophilicity (days)	Duration of hydrophobicity (days)
WT0	1	2–14
WT1	1–8	9–14
WT2	1–8	9–14
WT3	1–8	9–14
WT7	1–7	8–14
WT14	1–5	6–14

modify the PDMS surface of the microfluidic device, the originally hydrophobic surface of PDMS is modified to the partially hydrophilic–hydrophobic surface where its surface wettability can be altered and controlled by the water treatment. The recovery time from the hydrophilic surface to the hydrophobic is used as an indicator to control the surface wettability. Fig. 3 shows the WCA of the modified PDMS with Pluronic solution of $4.0 \mu\text{L g}^{-1}$ where WT0 is the sample without water treatment and WT1, WT2, WT3, WT7 and WT14 are the samples with water treatment for 1, 2, 3, 7 and 14 days, respectively. When the WCA with respect to the sample surface in case of water treatment is measured, such a sample is taken from water and blown with air until dried. Once the sample is dry, the WCA is measured immediately on which day it is counted as the first day. After that, the sample is stored in air. The WCA of the stored sample is daily measured for 14 days in order to study the stability of hydrophilic properties duration and the recovery of the hydrophobic surface when the sample experiences the water treatment at different time.

In Fig. 3, WT0 is the reference case where the WCA with no water treatment is 53.5° on the first day and increases up to 102.9° after 14 days. The hydrophilicity of WT0 can recover to the hydrophobic surface within 2 days. With the water treatment, the WCA of WT1 is 44.1° after one day in water which is the lowest one compared to other cases while the WCA of WT14 is 51.4° after 14 days in water which is the highest one because Pluronic dissolves in water and the oligomer of Pluronic inside PDMS is reduced after the sample is immersed in water for such a long time. Therefore, the surface of the sample with water treatment is hydrophilic up to 14 days according to the present result as long as the sample is immersed in water. After the samples are taken from water, Table 1 reveals that the hydrophilic surfaces of WT1, WT2 and WT3 samples require 9 days to recover to the hydrophobic surface whereas the surfaces of WT7 and WT14 samples become hydrophobic within 8 and 6 days, respectively. The WT1 sample will be investigated further because its contact angle is lowest and its recovery time from hydrophilic to hydrophobic surface is 9 days which is relatively long compared to other cases while its water treatment duration is shortest.

After 9 days of being exposed to air, the surface of the WT1 sample recovers from the hydrophilic to hydrophobic. The hydrophilic surface treatment is a process that the recovery of hydrophobic surface back to the hydrophilic surface is modified after being immersed in water. The effect of the hydrophilic

**Fig. 4** Water contact angles of the WT1 sample after the hydrophilic surface treatment within 24 hours.

surface treatment on the WCA is studied. Fig. 4 shows the WCA of the WT1 sample after the hydrophilic surface treatment from 0 min to 24 hours. At the beginning (0 min), the WCA of the WT1 sample is 90.2° . The hydrophilic surface treatment (immersed in water) for 30 min can modify the recovered hydrophobic surface of the WT1 sample back to the hydrophilic surface with the WCA of 84.1° . The WCA of the WT1 sample continually reduces when the duration of the water immersion is longer. Its WCA is 68.7° after being immersed in water for 24 hours.

Up to this stage, a new process for the surface preparation of a microfluidic device to generate water-in-oil-in-water double emulsion droplets is proposed in the present work. The microfluidic device is fabricated by using the permanent chemical coating modification with Pluronic surfactant solution concentration of $4.0 \mu\text{L g}^{-1}$ (W4 sample). This microfluidic device is processed with water treatment for one day (WT1) by flowing the deionized water (DIW) into the microfluidic device through all micro-channels and trapping the DIW inside the microfluidic device for a day in order to draw the oligomer of Pluronic towards the wetted surface of micro-channels and hence all wetted surfaces become hydrophilic (WCA = 44.1°) as shown in Fig. 5(a). After that, the DIW is drained out of this microfluidic device and the device is exposed to the ambient air for 9 days in order to recover its hydrophobic surface (WCA = 90.2°) as shown in Fig. 5(b). Finally, this microfluidic device is prepared for use to generate water-in-oil-in-water double emulsion droplets by continuously injecting two fluids (mineral oil and DIW) at the volume flow rate of $60 \mu\text{L h}^{-1}$ into the continuous phase inlets of two junctions for more than 30 min as shown in Fig. 5(c). The mineral oil flows into the left junction in order to maintain the hydrophobic surface (WCA = 90.2°) while the DIW flows into the right junction in order to modify the hydrophobic surface back to the hydrophilic one (WCA < 84.1°). The outlet of the micro-channel at the right junction is designed to be wider than the width of the middle micro-channel between the left junction and the right junction in order to ensure its lower pressure drop. The DIW always flows to the far right outlet and never flows toward the left junction. Although some small amount of mineral oil may flow to the right junction, the micro-droplets of mineral oil are enclosed by the DIW so that the mineral oil never contacts the surface of



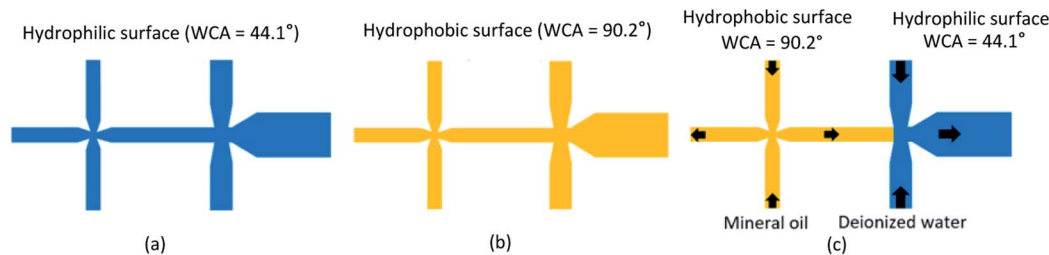


Fig. 5 Process for surface preparation of a microfluidic device to generate water-in-oil-in-water double emulsion droplets. (a) Micro-channels with Pluronic surfactant solution with a concentration of $4.0 \mu\text{L g}^{-1}$ after water treatment for 24 hours. (b) Micro-channels exposed to air longer than 9 days. (c) Micro-channels without hydrophilic surface treatment at the left junction and with hydrophilic surface treatment for more than 30 min at the right junction.

Table 2 Experimental conditions for water-in-oil-in-water double emulsion droplet generation at various Q_3 , Q_r and f_r

Condition	Q_3 ($\mu\text{L h}^{-1}$)	Q_r	f_r
1	100	5	0.73
2	120	6	0.85
3	140	7	0.96
4	150	7.5	1.02
5	160	8	1.08
6	180	9	1.19
7	200	10	1.30

microchannel at the right junction or after and hence no effect on surface wettability there.

Generation of w/o/w double emulsion droplets

In this section, the microfluidic device obtained from Section 3.2 is ready for generation of water-in-oil-in-water double emulsion droplets where the surface property of junction 1 is hydrophobic ($\text{WCA} = 90.2^\circ$) whereas the junction 2 is hydrophilic ($\text{WCA} < 84.1^\circ$). At junction 1, the water-in-oil droplets are generated for which the DIW is mixed with the red-color dye at the ratio of 1% w/w for $Q_1 = 20 \mu\text{L h}^{-1}$ and the mineral oil is mixed with Span 80 at the ratio of 0.5% w/w for $Q_2 = 20 \mu\text{L h}^{-1}$. At junction 1, $Q_1 = Q_2$. After junction 1, the water-in-oil droplets are delivered to junction 2 for encapsulation with the DIW mixed with Triton X-100 at the ratio of 2% w/w in order to obtain the water-in-oil-in-water droplets. At junction 2, the volume flow rate Q_3 of the DIW mixed with Triton X-100 is an important parameter because Q_3 affects the efficiency of encapsulation. In addition, at junction 2, the flow rate ratio (Q_r) is defined as the ratio of the continuous phase flow rate to the dispersed phase flow rate (Q_c/Q_d).

The present work proposes the principle of determining Q_3 to obtain the highest efficiency for encapsulation. The main principle is to equate the droplet generation frequency (f) of two junctions in terms of the dimensionless Strouhal number (St) defined in eqn (1):

$$St = \frac{fD_h}{U} \quad (1)$$

where f is the frequency of droplet generation (Hz), U is the droplet velocity (m s^{-1}) and D_h is the hydraulic diameter of each junction outlet (m). Equating the Strouhal number of two junctions yields the following frequency ratio:

$$f_r = \frac{f_2}{f_1} = \frac{U_2 D_{h2}}{U_1 D_{h1}} \quad (2)$$

where f_r is the droplet generation frequency ratio and the subscripts 1 and 2 denote the junctions 1 and 2, respectively. In principle, the highest encapsulation efficiency is obtained when $f_r = 1$. Whether $f_r < 1$ or $f_r > 1$, the encapsulation efficiency is lower.

This work demonstrates the experiment of generating water-in-oil-in-water double emulsion droplets at various droplet generation frequency ratios and flow rate ratios. Table 2 provides a list of 7 experimental conditions by varying the volume flow rate, Q_3 , of the DIW mixed with Triton X-100 at junction 2 from 100 to 200 $\mu\text{L h}^{-1}$ in order to cover a range of the flow rate ratios of 5–10 and the droplet generation frequency ratios of 0.73–1.30.

Fig. 6(a) shows the experimental results of water-in-oil-in-water droplet generation where the water-in-oil droplet generation at junction 1. Fig. 6(b) displays the water-in-oil-in-water droplet generation at junction 2 at various droplet generation frequency ratios. Fig. 6(c) shows the frame locations where the pictures shown in Fig. 6(a) and (b) are taken. It reveals that the microfluidic device after surface modification with permanent chemical coating can effectively generate water-in-oil droplets at junction 1. These water-in-oil droplets are continuously delivered to junction 2. At junction 2, the volume flow rate Q_3 of the DIW mixed with Triton X-100 is varied to generate water-in-oil-in-water droplets at various droplet generation frequency ratio as shown in Fig. 6(b). It is found that the optimal encapsulation takes place when $f_r = 1.02$ with $Q_3 = 150 \mu\text{L h}^{-1}$ where all DIW droplets with red color are encapsulated inside the mineral oil droplet while at other droplet generation frequency ratios the encapsulation cannot occur for all water-in-oil droplets. Moreover, some encapsulated droplets become unstable later leading to encapsulation failure.

Fig. 7 shows the water-in-oil-in-water droplet encapsulation efficiency in the primary vertical axis and the droplet diameter in the secondary vertical axis at various droplet generation frequency ratios together with one sample of droplet image per



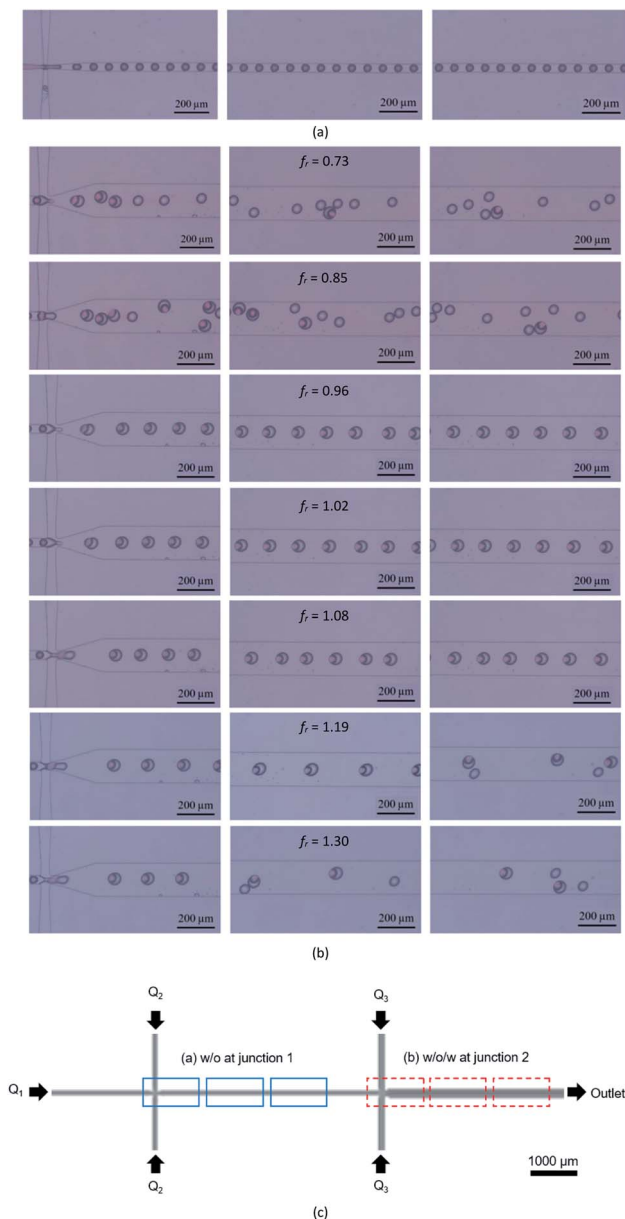


Fig. 6 Droplet generation in the microfluidic channel (a) junction 1 for water-in-oil droplets, (b) junction 2 for water-in-oil-in-water droplets and (c) locations where the images are captured.

each frequency ratio, where the highest efficiency is 92.4% at $f_r = 1.02$. At this frequency ratio, the average outer and inner diameters of water-in-oil-in-water double emulsion droplets are 75.0 and 57.7 μm , respectively. Note that the uncertainty error is less than 1 μm . The effect of flow rate ratios on the resultant emulsion is also investigated and the results in Fig. 7(a) reveals that the outer diameter of double emulsion droplets increases with increasing flow rate ratio while their inner diameter is more or less unaltered. The droplet encapsulation efficiency and the averaged outer and inner droplet diameters are determined by the following procedure: (1) drop a certain amount of droplets onto the glass slide and let the droplets settle down into a form of monolayer, (2) take the image of droplets by the

optical microscope (OLYMPUS BX51M) with a magnification of 50 \times using the CCD camera (HAYEAR, 5.0MP CMOS) with the resolution of 1280 \times 720 pixels, (3) calculate the droplet encapsulation efficiency defined as the number of double emulsion droplets per the total number of droplets and average the droplet encapsulation efficiency from 10 pictures per frequency ratio, and (4) use the S-EYE software to measure the average outer and inner droplet diameters from 50 random droplets per image.

Experimental

Materials and equipment

PDMS (Dow Corning, Sylgard 184 Elastomer Kit) is a material used to fabricate the microfluidic device. The micro-channel surface is modified by permanent chemical coating for which the surfactant solution is made of Pluronic F-127 (Sigma Aldrich) and ethanol (Sigma Aldrich). The water-in-oil-in-water droplets is composed of (1) DIW mixed with red-color dye at the ratio of 1.0% w/w for the inner dispersed phase (Q_1) in order to enhance the flow visualization inside the micro-channel, (2) mineral oil (SKYDD, AA-1086768) mixed with Span 80 (Sigma Aldrich) at the ratio of 0.5% w/w for the middle continuous phase (Q_2) and (3) DIW mixed with Triton X-100 (Sigma Aldrich) at the ratio of 2.0% w/w for the outer continuous phase (Q_3).

The solutions of the inner dispersed phase, the middle continuous phase and the outer continuous phase are injected into the microfluidic device through silicone tubes (Cole Parmer, 0.02" i.d.) and disposable syringes (NIPRO, 1.0 mL) using three syringe pumps (NE-1000, New Era Pump System, Inc.) at the flow rates over a range of 10–200 $\mu\text{L h}^{-1}$. The image of generated droplets and the monitoring screens at two junctions inside the micro-channels are captured by the optical microscope (OLYMPUS BX51M) with CCD camera (HAYEAR, 5.0MP CMOS). The diameter of droplets is measured on the glass slide by using the S-EYE software using 50 random samples of droplets.

Microfluidic device design for double emulsion droplet generation

The microfluidic device for double emulsion droplet generation is designed by using the flow focusing micro-channel technique. The schematic diagram of the microfluidic device is shown in Fig. 8. There are two main junctions in this microfluidic device: junction 1 for water-in-oil droplet generation and junction 2 for water-in-oil-in-water droplet generation. At junction 1, the surface property is hydrophobic (yellow) with the micro-channel width of 50 μm of W_1 , W_2 and W_{m1} and all the micro-channel widths are gradually reduced to be 20 μm at this junction. The water-in-oil droplet are generated by junction 1 are delivered as the dispersed phase to junction 2 in order to generate the double emulsion water-in-oil-in-water droplets. At junction 2, the micro-channel widths of W_{m1} , W_3 and W_{m2} are 50, 100 and 200 μm , respectively. The micro-channel widths are gradually reduced to 50 μm at the junction. Note that the depth



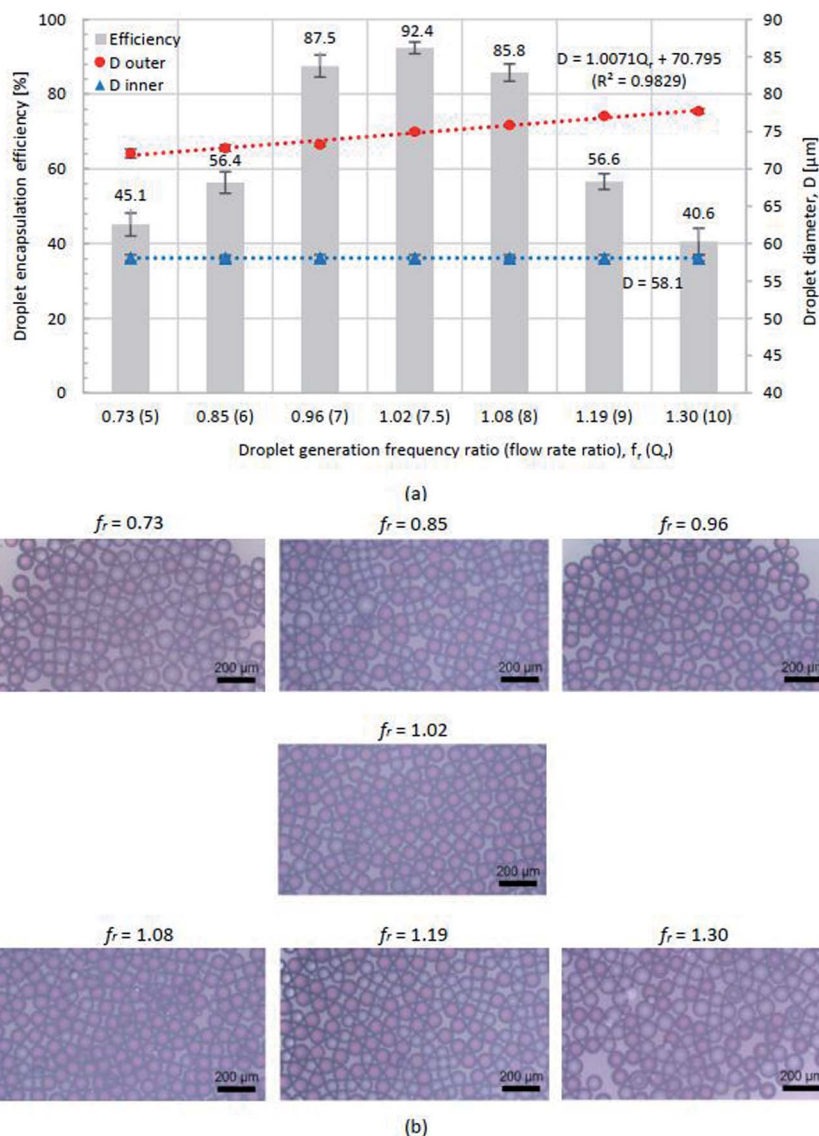


Fig. 7 (a) Droplet encapsulation efficiency (primary vertical axis) and droplet diameter (secondary vertical axis) and (b) images of water-in-oil-in-water droplets at $f_r = 0.73$ –1.30.

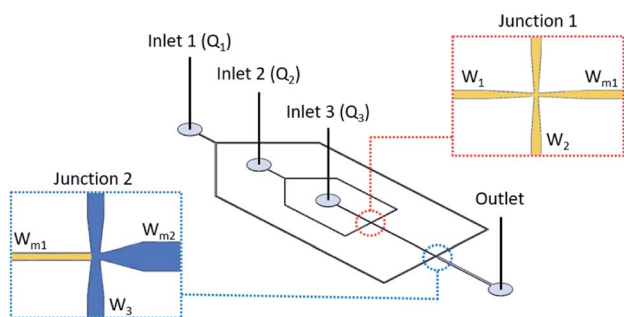


Fig. 8 Schematic diagram of the microfluidics device for double emulsion droplet generation with the flow-focusing micro-channel.

of the micro-channel in the microfluidic device is fixed at 100 μm .

Microfluidic device fabrication and surface modification

There are two main processes to fabricate the microfluidic device for double emulsion droplet generation: the fabrication of the silicon master (Si mold) and the casting of the PDMS microfluidic device. For the Si mold fabrication, a 6-inch diameter Si wafer is cleaned by immersed in a piranha acid solution 70% H_2SO_4 : 30% H_2O_2 at volume ratio of 4 : 1 heated at 120 $^\circ\text{C}$ for 10 min in order to remove organic contaminants from the surface and rinsed with DIW at 25 $^\circ\text{C}$ for 10 min. Then, the sample is blow-dried with pure nitrogen gas. Then, the Si wafer is spin-coated with the hexamethyldisilazane (HMDS) mold releasing agent and baked at 90 $^\circ\text{C}$ for 90 seconds to improve the photoresist (PR) adhesion to the oxidized Si-wafer surface. A commercially positive PR, PF1-34A (Sumitomo Corporation), is spin-coated at 1000 rpm for 20 s in order to obtain a thickness of 2.0 μm on the Si wafer. The patterned



channel is prepared by a conventional photolithography using a contact mask aligner (EVG 620, EV Group). A photomask with feature sizes ranging from 20 μm to 200 μm is used. The spin-coated wafer is then exposed to the 365 nm UV-light through a photomask. The UV-light intensity is 40 mW cm^{-2} and the exposure time is 5 s. The Si wafer is post-exposure baked at 110 $^{\circ}\text{C}$ for 100 s in order to reduce the standing wave effect at sidewall of PR patterns, then developed in SD-W developer (Sumitomo Corporation) for 75 s, and hard baked at 120 $^{\circ}\text{C}$ for 80 seconds. After that, the photo-patterned Si wafer is etched by deep reactive ion etching (DRIE) using $\text{SF}_6/\text{C}_4\text{F}_8$ gases (200/5 sccm, ICP/RIE: 2000/10 W, 8 s). The remaining PR is removed by oxygen plasma. Finally, the Si-master with 100 μm etch depth is obtained.

The PDMS microfluidic device is fabricated by the soft lithography process with the surface modification using permanent chemical coating. The surfactant solution used to mix with PDMS for surface modification is made of Pluronic F-127 of 200 grams and ethanol of 1.0 mL in proportion. This surfactant solution is mixed in a vortex mixer for 2 min and then heated up to 45 $^{\circ}\text{C}$ for 1 h. A PDMS precursor and a curing agent are mixed at the ratio of 10 : 1 w/w, together with the surfactant solution at various ratios in order to modify the PDMS surface from hydrophobic to hydrophilic. After that, the PDMS mixture is poured onto the Si master, degassed in vacuum chamber for 10 min and cured at 75 $^{\circ}\text{C}$ for 90 min and stored for 12 h. Then, the cured PDMS is released from the Si master, cut and punched to connect with silicone tubes. The PDMS cavity side obtained is directly bonded to a PDMS flat sheet after the surface treatment with the oxygen plasma (O_2 gas flow rate: 40 sccm, RF power: 30 W, etching time 90 s).

Conclusions

This research work proposes the process of developing the microfluidic device with surface modification using permanent chemical coating for the generation of double emulsion microdroplets with the flow-focusing micro-channel technique. The surface of this microfluidic device is modified from the hydrophobic surface to the partially hydrophilic-hydrophobic surface whose property is hydrophobic at normal condition like a bulk PDMS. For usage, this partially hydrophilic-hydrophobic surface can be changed from hydrophobic to hydrophilic by the water treatment. This permanent chemical coating makes the surface wettability preparation convenient and any specific surface region can be selected for surface modification. In this work, the Pluronic surfactant solution concentration of 4 $\mu\text{L g}^{-1}$ is found to be the most suitable one because its percent transmission is not much different from that of PDMS without surface modification.

After surface modification, the microfluidic device requires 9 days to recover the hydrophobic surface. When the microfluidic device is set up to generate double emulsion droplets, the water treatment is required by injecting the deionized water into micro-channels, where their surfaces need modifying from hydrophobic to hydrophilic, for 30 min. In this work, the water-in-oil-in-water double emulsion droplets are successfully

generated using this microfluidic device with the droplet encapsulation efficiency of 92.4%. The optimal condition for effectively generating double emulsion droplets is achieved by adjusting the flow rate Q_3 to equate the droplet generation frequencies at two junctions ($f_r = 1$) in order to ensure the maximum droplet encapsulation efficiency. This microfluidic device is convenient for double emulsion droplet generation and also suitable for biomedical applications with complex hydrophilic and hydrophobic patterns.

Conflicts of interest

There are no conflicts to declare.

Acknowledgements

The authors would like to gratefully thank the researchers of Thai Microelectronics Center (TMEC), National Electronics and Computer Technology Center (NECTEC), Thailand and Department of Physiology, Faculty of Medicine, Siriraj Hospital, Mahidol University (MU), Thailand for their helpful assistance. The project is financially supported by National Science and Technology Development Agency (NSTDA), Thailand [Grant No. P-16-50098] and Faculty of Medicine, Siriraj Hospital, MU, Thailand [Grant No. r015936004]. Thailand Graduate Institute of Science and Technology (TGIST), NSTDA, Ministry of Higher Education, Research and Innovation (MHESI) [Grant No. TG-44-21-61-014D] is greatly acknowledged for the PhD scholarship of the first author AK. Special thanks go to Dr Therdthai Thienthong for fruitful discussion on Strouhal number.

Notes and references

- 1 D. Vasiljevic, J. Parojcic, M. Primorac and G. Vuleta, *Int. J. Pharm.*, 2006, **309**, 171–177.
- 2 X. Gong, S. Peng, W. Wen, P. Sheng and W. Li, *Adv. Funct. Mater.*, 2009, **19**, 292–297.
- 3 K. K. Brower, C. C. Crumpton, S. Klemm, B. Cruz, G. Kim, S. G. K. Calhoun, L. Nichols and P. M. Fordyce, *Lab Chip*, 2020, **20**, 2062–2074.
- 4 K. Hettiarachchi, H. Kim and G. W. Faris, *Microfluid. Nanofluid.*, 2012, **13**, 967–975.
- 5 K. Liu, Y. Deng, N. Zhang, S. Li, H. Ding, F. Guo, W. Liu, S. Guo and X. Z. Zhao, *Microfluid. Nanofluid.*, 2012, **13**, 761–767.
- 6 Y. Ding, J. Choo and A. J. DeMello, *Microfluid. Nanofluid.*, 2017, **21**, 58.
- 7 R. Guo, C. G. Yang and Z. R. Xu, *Microfluid. Nanofluid.*, 2017, **21**, 157.
- 8 Z. Vaezi, M. Sedghi, M. Ghorbani, S. Shojaeilangari, A. Allahverdi and H. N. Manesh, *Microfluid. Nanofluid.*, 2020, **24**, 48.
- 9 K. Wang, K. Qin, T. Wang and G. Luo, *RSC Adv.*, 2015, **5**, 5474–6470.
- 10 S. R. Doonan, M. Lin, D. Lee, J. Lee and R. C. Bailey, *Microfluid. Nanofluid.*, 2020, **24**, 50.



- 11 H. C. Shum, D. Lee, I. Yoon, T. Kodger and D. A. Weitz, *Langmuir*, 2008, **24**, 7651–7653.
- 12 Y. Zheng, Z. Yu, R. M. Parker, Y. Wu, C. Abell and O. A. Scherman, *Nat. Commun.*, 2014, **5**, 5772.
- 13 B. Kim, T. Y. Jeon, Y. K. Oh and S. H. Kim, *Langmuir*, 2015, **31**, 6027–6034.
- 14 S. Deshpande, Y. Caspi, A. E. C. Meijering and C. Dekker, *Nat. Commun.*, 2016, **7**, 10447.
- 15 H. Lee, C. H. Choi, A. Abbaspourrad, C. Wesner, M. Caggioni, T. Zhu and D. A. Weitz, *ACS Appl. Mater.*, 2016, **8**, 4007–4013.
- 16 K. L. Thompson, S. P. Armes and D. W. York, *Langmuir*, 2011, **27**, 2357–2363.
- 17 M. S. Manga, O. J. Cayre, R. A. Williams, S. Biggs and D. W. York, *Soft Matter*, 2012, **8**, 1532–1538.
- 18 L. Zhang, Z. Liu, L. Y. Liu, J. L. Pan, F. Luo, C. Yang, R. Xie, X. J. Ju, W. Wang and L. Y. Chu, *ACS Appl. Mater. Interfaces*, 2018, **10**, 44092–44101.
- 19 K. Wang, Y. C. Lu, J. H. Xu, J. Tan and G. S. Luo, *Microfluid. Nanofluid.*, 2009, **6**, 557–564.
- 20 K. Wang, Y. C. Lu, J. H. Xu, J. Tan and G. S. Luo, *AIChE J.*, 2011, **57**, 2.
- 21 X. Wang, Y. Yong, Ch. Yang, Z. S. Mao and D. Li, *Microfluid. Nanofluid.*, 2014, **16**, 413–423.
- 22 M. Seo, C. Paquet, Z. Nie, S. Xua and E. Kumacheva, *Soft Matter*, 2007, **3**, 986–992.
- 23 N. Pannacci, H. Bruus, D. Bartolo, I. Etchart, T. Lockhart, Y. Hennequin, H. Willaime and P. Tabeling, *Phys. Rev. Lett.*, 2008, **101**, 164502.
- 24 A. R. Abate, J. Thiele, M. Weinhart and D. A. Weitz, *Lab Chip*, 2010, **10**, 1774–1776.
- 25 W. C. Bauer, M. Fischlechner, C. Abell and W. T. S. Huck, *Lab Chip*, 2010, **10**, 1814–1819.
- 26 H. H. Lin, S. C. Chang and Y. C. Su, *Microfluid. Nanofluid.*, 2010, **9**, 1091–1102.
- 27 A. R. Abate, J. Thiele and D. A. Weitz, *Lab Chip*, 2011, **11**, 253–258.
- 28 N. N. Deng, Z. J. Meng, R. Xie, X. J. Ju, C. L. Mou, W. Wang and L. Y. Chu, *Lab Chip*, 2011, **11**, 3963.
- 29 J. Thiele and S. Seiffert, *Lab Chip*, 2011, **11**, 3188.
- 30 S. Hwang, C. H. Choi and C. S. Lee, *Macromol. Res.*, 2012, **20**, 4.
- 31 P. Jankowski, D. Ogonczyk, L. Derzsi, W. Lisowski and P. Garstecki, *Microfluid. Nanofluid.*, 2013, **14**, 767–774.
- 32 B. Wu, H. Q. Gong and R. Zhang, *Microfluid. Nanofluid.*, 2014, **16**, 1069–1074.
- 33 N. N. Deng, C. L. Mou, W. Wang, X. J. Ju, R. Xie and L. Y. Chu, *Microfluid. Nanofluid.*, 2014, **17**, 967–972.
- 34 S. Li, X. Gong, C. S. Mc Nally, M. Zeng, T. Gaule, C. Anduix-Canto, A. N. Kulak, L. A. Bawazer, M. J. McPhersonb and F. C. Meldrum, *RSC Adv.*, 2016, **6**, 25927–25933.
- 35 H. Hirama, S. Wada, J. Shimamura, Y. Komazaki, T. Inoue and T. Torii, *Microfluid. Nanofluid.*, 2017, **21**, 91.
- 36 B. Cai, T. T. Ji, N. Wang, X. B. Li, R. X. He, W. Liu, G. Wang, X. Z. Zhao, L. Wang and Z. Wang, *Lab Chip*, 2019, **19**, 422–431.
- 37 Q. Q. Liao, S. K. Zhao, B. Cai, R. X. He, L. Rao, Y. Wu, S. S. Guo, Q. Y. Liu, W. Lui and X. Z. Zhao, *Sens. Actuators, A*, 2018, **279**, 313–320.
- 38 S. Nawar, J. K. Stolaroff, C. Ye, H. Wu, D. T. Nguyen, F. Xin and D. A. Weitz, *Lab Chip*, 2020, **20**, 147.
- 39 L. Nan, Y. Cao, S. Yuan and H. C. Shum, *Microsyst. Nanoeng.*, 2020, **6**, 70.
- 40 A. Schmit, L. Courbin, M. Marquis, D. Renard and P. Panizza, *RSC Adv.*, 2014, **4**, 28504.
- 41 T. Si, H. Feng, X. Luo and R. X. Xu, *Microfluid. Nanofluid.*, 2015, **18**, 967–977.
- 42 W. Wang, M. J. Zhang and L. Y. Chu, *Curr. Opin. Pharmacol.*, 2014, **18**, 35–41.
- 43 M. A. Levenstein, L. A. Bawazer, C. S. Nally, W. J. Marchant, X. Gong, F. C. Meldrum and N. Kapur, *Microfluid. Nanofluid.*, 2016, **20**, 143.
- 44 Z. Che, T. N. Wong and N. T. Nguyen, *Microfluid. Nanofluid.*, 2017, **21**, 8.
- 45 L. Hou, Y. Ren, Y. Jia, X. Chen, X. Deng, Z. Tang, Q. Hu, Y. Tao and H. Jiang, *Microfluid. Nanofluid.*, 2017, **21**, 60.
- 46 M. Michelona, Y. Huang, L. G. Torrec, D. A. Weitz and R. L. Cunha, *Chem. Eng. J.*, 2019, **366**, 27–32.
- 47 R. Song, M. S. Abbasi and J. Lee, *Microfluid. Nanofluid.*, 2019, **23**, 92.
- 48 Z. Wu and K. Hjort, *Lab Chip*, 2009, **9**, 1500–1503.

